Energy Spectrum of Carriers in a Kane-type Semiconductor Anti-wire

Seyfettin Çakmak

Department of Physics, University of Suleyman Demirel, Isparta 32260, Turkey

Reprint requests to Dr. S. C.; E-mail: scakmak@fef.sdu.edu.tr

Z. Naturforsch. **60a,** 593 – 598 (2005); received March 29, 2005

The electronic states of a Kane-type semiconductor anti-wire with and without a magnetic field are theoretically investigated. The eigenvalues and eigenstates of Kane's Hamiltonian are obtained. The calculations are performed for a hard-wall confinement potential, and electronic states are obtained as functions of the magnetic field applied along the cylinder axis. The size dependences of the effective g-value in InSb for electrons and light holes are calculated. The effective g-values of the electrons and light holes decreased with decreasing anti-wire radius.

Key words: Nanostructures; Spin-orbital Coupling; g-Factor.

1. Introduction

Studies of the basic properties of low-dimensional (quantum dots, wires, wells, anti-wires) electron distributions, that are mostly realized in semiconductor structures, have recently been in the forefront of research in condensed matter physics as a result of technological advancement in two-dimensional nanostructures [1, 2]. The energy spectrum of carriers in quantum dots and quantum wires was theoretically investigated in [3 – 6]. The electron energy states in an uniform magnetic field directed along the quantum wire were studied using a free electron model [3]. In [4] the energy spectrum of an electron confined in a quantum wire by an infinite square potential by using effective mass approximation both with and without an axial magnetic field was calculated. The energy levels of an electron confined in a barrier like multilayer quantum wire structure with a perpendicular magnetic field along the z-direction in cylindrical coordinates are derived in [5]. Magneto optical properties of quantum dots in semiconductors have been considered for the model of hard-wall confinement taking into account the real band structure of InSb-type materials (narrow energy gap and strong spin-orbital interaction) [6]. The spin-orbital interaction and the contribution of the electrons to the g-factor were detailed in [7, 8]. For calculating the electron g-values in [7], the three band Kane's model was used, where the nonparabolicity of the electron and light hole bands and the complex structure of the valence bands were simultaneously taken into account. This model describes the energy band structure around the Γ point of the Brillouin zone very well. In a paper of Masale, the energy spectrum of a single electron confined near a cylindrical cavity is determined within the effective mass approximation as a function of the applied parallel magnetic field [9]. In [9], the energy spectrum as function of the magnetic field explained that for small radii, the $m \leq -3$ states all fall in the infinitely degenerate ground states, where as for a larger radius the energy eigenvalues showed a somewhat parabolic variation with the magnetic field. In [10], a confined electronic system is modeled as an electron moving outside a cylinder of radius a. The magnetic field configuration for it's Landau states and for the Aharonov-Bohm effect on such states was given; then the respective Schrödinger equations were successfully formulated and solved. They named the confined electronic system an antidot. Perhaps a better name as a quantum anti-wire. The simple parabolic energy bands omit the spin effect. However the experimental advantages of using narrow gap semiconductors for the reduced dimensionality make it necessary to take into account the real band structure of materials. When considering the nonparabolicity of the electron dispersion in narrow and medium gap semiconductors, the coupling of the conduction and valence bands should be taken into account. This is the purpose of our present work.

In this work, using Kane's three-band model including the conduction band, and light and spin-orbital hole bands, the electron spectrum with and without magnetic field, and electron and light hole effective g-factors of anti-wire are calculated. The system considered

here might simply be a very long cylindrical cavity of radius R etched out of a bulk composite semiconductor material. We take the potential of the anti-wire to be infinitive at the boundary and zero elsewhere. We omit the free-electron term in the diagonal part and the Pauli spin term, as they give only small contributions to the effective mass and the spin g-value of electrons and light holes in InSb.

The Kane problem, i.e. determination of the energy spectrum taking into account the interaction of three bands, conduction band, light hole band and spin-orbital splitting band, in a magnetic field was considered in a paper of Bowers and Yafed [11].

In the three-band Kane's Hamiltonian the valence and conduction bands interaction is taken into account via the only matrix element P (so called Kane's parameter). The system of Kane equations, including the nondispersional heavy hole bands, has the form [12, 13]

$$-EC_1 - \frac{Pk_-}{\sqrt{2}}C_3 + \sqrt{\frac{2}{3}}Pk_zC_4 + \frac{Pk_+}{\sqrt{6}}C_5 + \frac{Pk_z}{\sqrt{3}}C_7 + \frac{Pk_+}{\sqrt{3}}C_8 = 0, \tag{1}$$

$$-EC_2 - \frac{Pk_-}{\sqrt{6}}C_4 + \sqrt{\frac{2}{3}}Pk_zC_5 + \frac{Pk_+}{\sqrt{2}}C_6 + \frac{Pk_-}{\sqrt{3}}C_7 - \frac{Pk_z}{\sqrt{3}}C_8 = 0, \tag{2}$$

$$-\frac{Pk_+}{\sqrt{2}}C_1 - (E+E_g)C_3 = 0, \tag{3}$$

$$\sqrt{\frac{2}{3}}Pk_zC_1 - \frac{Pk_+}{\sqrt{6}}C_2 - (E+E_g)C_4 = 0, \tag{4}$$

$$\sqrt{\frac{2}{3}}Pk_zC_2 + \frac{Pk_-}{\sqrt{6}}C_1 - (E+E_g)C_5 = 0, \tag{5}$$

$$\frac{Pk_-}{\sqrt{2}}C_2 - (E+E_g)C_6 = 0, \tag{6}$$

$$\frac{Pk_z}{\sqrt{3}}C_1 + \frac{Pk_+}{\sqrt{3}}C_2 - (\Delta+E+E_g)C_7 = 0, \tag{7}$$

$$\frac{Pk_-}{\sqrt{3}}C_1 - \frac{Pk_z}{\sqrt{3}}C_2 - (\Delta+E+E_g)C_8 = 0. \tag{8}$$

Here P is the Kane parameter, E_g the band gap energy, Δ the value of spin-orbital splitting and $k_\pm = k_x \pm ik_y$, $\boldsymbol{k} = -i\nabla$.

2. Zero Magnetic Field

Substituting (3) – (8) into (1) and (2) we obtain

$$\left\{-E - \frac{P^2}{3}\left[\frac{2}{E+E_g} + \frac{1}{E+E_g+\Delta}\right]\boldsymbol{\Delta}_3\right\}C_{1,2} = 0, \tag{9}$$

where $\boldsymbol{\Delta}_3$ is the three dimensional Laplacien.

In cylindrical coordinates, the eigenfunction is

$$C_{1,2} = A\exp(im\phi + ik_z z)R_{1,2}(\rho), \tag{10}$$

where A is a normalization factor, k_z is the axial wavenumber and m the azimuthal quantum number. The radial function $R(\rho)$ is found to satisfy the following differential equation:

$$\left\{\frac{P^2}{3}\left(\frac{2}{E+E_g} + \frac{1}{E+E_g+\Delta}\right) \cdot \left[\frac{d^2}{d\rho^2} + \frac{1}{\rho}\frac{d}{d\rho} - \frac{m^2}{\rho^2} - k_z^2\right] + E\right\}R_{1,2}(\rho) = 0. \tag{11}$$

Equation (11) can be rewritten in the form

$$\left(\frac{d^2}{d\rho^2} + \frac{1}{\rho}\frac{d}{d\rho} - \frac{m^2}{\rho^2} + \chi^2\right)R_{1,2}(\rho) = 0, \tag{12}$$

where

$$\chi^2 = \frac{3}{P^2}\frac{E(E+E_g)(E+E_g+\Delta)}{(3E+3E_g+2\Delta)} - {k_z}^2. \tag{13}$$

Equation (12) is Bessel's differential equation [14], the solution of (11) at infinity is

$$R_{1,2}(\rho) = CY_m(\chi\rho), \tag{14}$$

where Y_m is the second order Bessel function. For an infinite wall of radius R, the boundary condition is $R_{1,2}(R) = 0$, so the eigenvalue equation is

$$Y_m(\chi R) = 0. \tag{15}$$

Equations (13) and (15) together show that the radial eigenvalue spectrum is

$$\frac{E(E+E_g)(E+E_g+\Delta)}{3E+3E_g+2\Delta} = \left(\frac{z_{mp}^2}{R^2} + {k_z}^2\right)\frac{P^2}{3}, \tag{16}$$

where z_{mp} is the pth root of the mth Bessel function $Y(z)$.

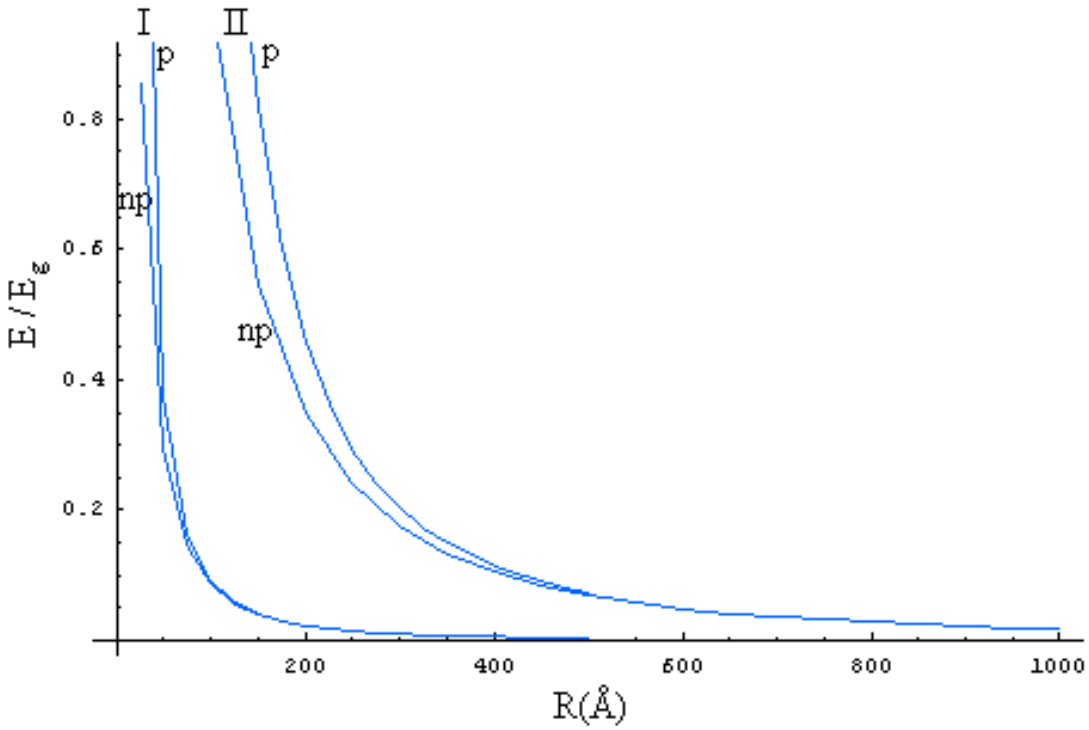

Fig. 1. The energy spectrum of electrons calculated as a function of the radius in an InSb anti-wire. I is for the first root of the Bessel differential equation, II is for the second root of the Bessel differential equation. p is for electrons with parabolic dispersion law, np for electrons with Kane's dispersion law (nonparabolic).

Equation (16) determines the energies of electrons, light holes, and the spin-orbital split-off band of holes in a Kane-type semiconductor anti-wire.

In Fig. 1, the dependencies of $E(R)$ for two cases are presented: a) electrons with parabolic dispersion law, b) electrons with Kane's dispersion law in an InSb anti-wire according to both the first and second roots of Bessel's differential equation. As it's seen in Fig. 1, with the increase of R, the electron energy levels in parabolic and nonparabolic cases become close to each other. At rather small values of R, the variance electron dispersion law becomes more important, and therefore the curves for $E(R)$ keep away from each other strongly in II compared to I. The following band parameters have been used for InSb: $E_{\mathrm{g}} = 0.2368$ eV, $\Delta = 0.810$ eV, $E_{\mathrm{P}} = 23.41$ eV, $E_{\mathrm{P}} = \left(\frac{2m_0}{\hbar^2}\right) P^2$, m_0 is the free-electron mass [15].

3. Applied Magnetic Field, Infinite Step

For an uniform magnetic field $\boldsymbol{H}$, directed along the z axis, the vector potential may be chosen in the form

$$\boldsymbol{A} = \left(-\frac{H_y}{2}, \frac{H_x}{2}, 0\right), \tag{17}$$

and $k_{\pm}$ has the forms

$$k_{\pm} \to k_{\pm} \pm \mathrm{i}\frac{1}{2}\lambda_H r_{\pm}, \tag{18}$$

where

$$r_{\pm} = x \pm \mathrm{i}y, \quad \lambda_H = \frac{eH}{\hbar c}. \tag{19}$$

Substituting (3)–(8) into (1) and (2), and using (19), (20), we obtain

$$\begin{pmatrix} -E + \dfrac{P^2}{3}\left(\dfrac{2}{E+E_{\mathrm{g}}} + \dfrac{1}{E+E_{\mathrm{g}}+\Delta}\right) \\ \qquad \cdot \left(-\nabla^2 + \lambda_H L_z + \dfrac{1}{4}\lambda_H^2 \rho^2\right) \\ \pm \dfrac{P^2 \lambda_H}{3}\left(\dfrac{1}{E+E_{\mathrm{g}}} - \dfrac{1}{E+E_{\mathrm{g}}+\Delta}\right) \end{pmatrix} C_{1,2} = 0, \tag{20}$$

where L_z is the z component of the angular momentum operator L, $\rho^2 = x^2 + y^2$.

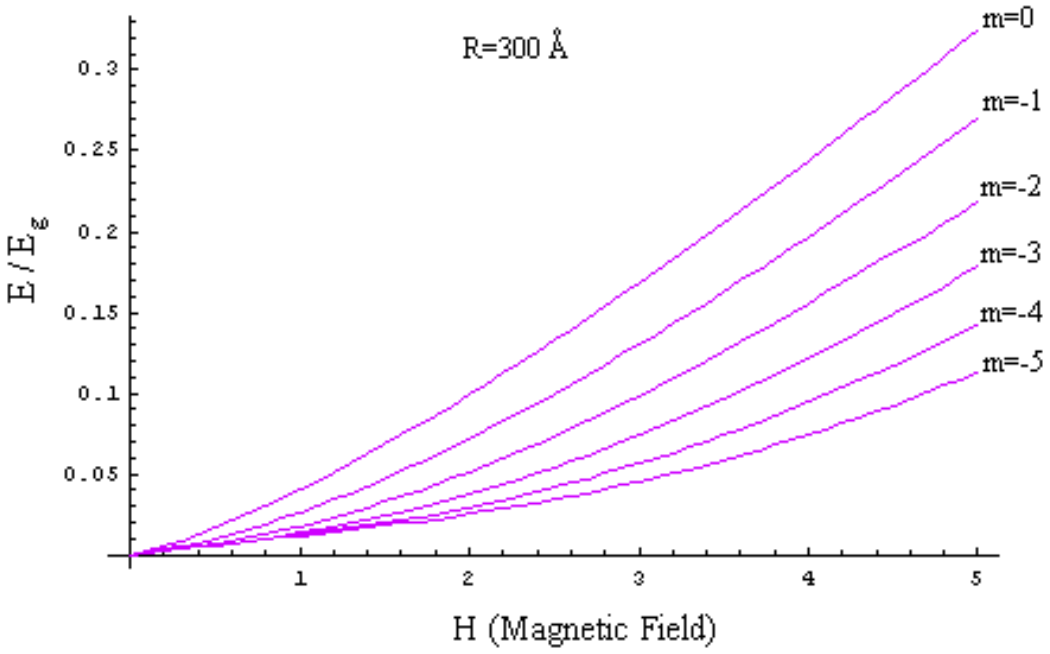

Fig. 2. Some of the lowest order $l_z = 0$, $k_z = 0$ electron energy eigenvalues as functions of the axial field $\boldsymbol{H}$ for $R = 300$ Å in an InSb-type anti-wire.

If to seek the solution of (21) in cylindrical coordinates in the form

$$C_{1,2} = A_{1,2} \exp(\mathrm{i}m\varphi + \mathrm{i}k_z z) \exp\left(-\frac{\xi}{2}\right) \xi^{\frac{|m|}{2}} \Phi_{1,2}(\xi), \tag{21}$$

we obtain for the radial function $\Phi(\xi)$:

$$\xi \frac{\mathrm{d}^2\Phi}{\mathrm{d}\xi^2} + (|m| + 1 - \xi)\frac{\mathrm{d}\Phi}{\mathrm{d}\xi} - \alpha_{1,2}\Phi = 0. \tag{22}$$

Equation (22) is the canonical form of Kummer's equation for the confluent hypergeometric function [16]. In (21), $\xi = \frac{\rho^2}{2l_H^2}$ is the dimensionless variable and l is the radial wavenumber. The solution of (22) is

$$\Phi(\xi) = U(\alpha_{1,2}, b, \xi), \tag{23}$$

where

$$\begin{aligned}\alpha_{1,2} = {} & \frac{1}{2} + \frac{m}{2} + \frac{|m|}{2} + \frac{1}{2}k_z^2 l_H^2 \\ & - \frac{3E}{\hbar\omega_0}\frac{(E+E_\mathrm{g})(E+E_\mathrm{g}+\Delta)}{(3E+3E_\mathrm{g}+2\Delta)E_\mathrm{p}} \\ & \pm \frac{\Delta}{2(3E+3E_\mathrm{g}+2\Delta)}.\end{aligned} \tag{24}$$

$\omega_0 = \frac{eH}{m_0 c}$ is the cyclotron frequency for free electrons, $l_H = \sqrt{\frac{\hbar c}{eH}}$ is the magnetic length and

$$b = |m| + 1 \tag{25}$$

are the parameters of the Kummer function in standard notation. The boundary conditions, which correspond to the infinite potential at $\rho = R$, are $C_{1,2} = 0$. These lead to the eigenvalue equations

$$U(\alpha_{1,2}, b, \frac{R^2}{2l_H^2}) = 0. \tag{26}$$

Equation (26) is just the eigenvalue problem solved by Çakmak et al. [17] for the case of a Kane-type quantum wire, except that here the function $U(\alpha_{1,2}, b, \xi)$ replaces $M(\alpha_{1,2}, b, \xi)$.

Figure 2 shows examples of the magnetic field dependence of the lowest order subbands for $l = 0$, $k_z = 0$ electron energy eigenvalues in an InSb anti-wire of radius $R = 300$ Å with infinite potential. The energy eigenvalues show a somewhat parabolic variation with the magnetic field and a more pronounced separation in energy of the $m \leq 0$ states of spin negative values. This is the same as in the energy of the $m \leq 0$ states of

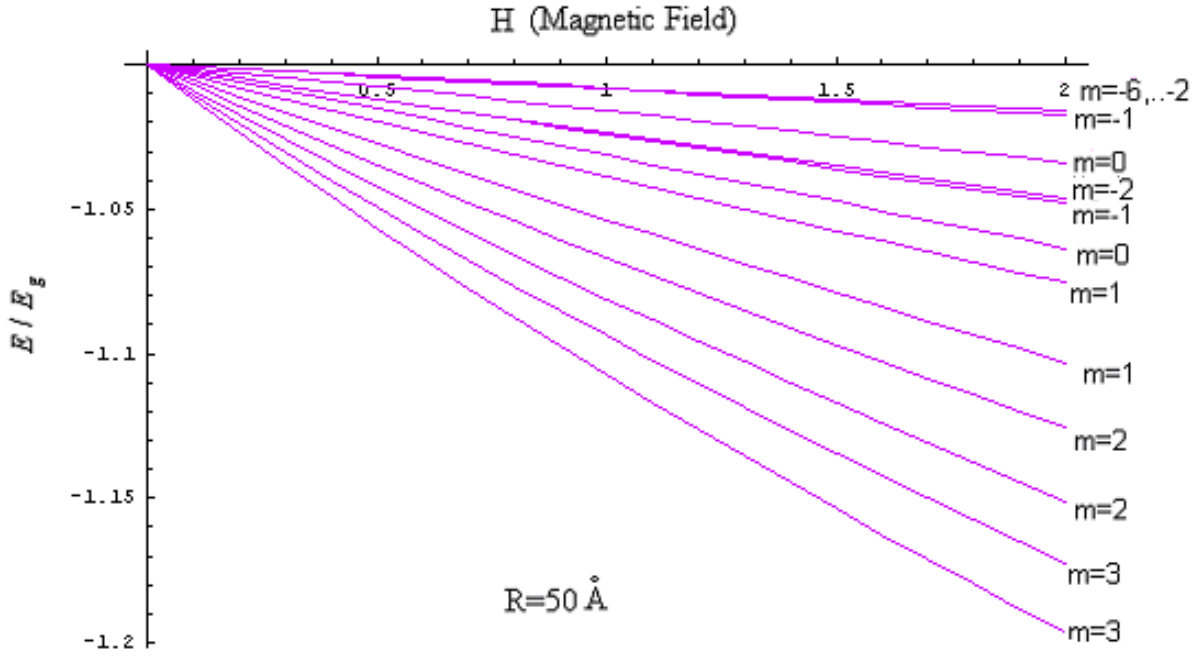

Fig. 3. Some of the lowest order $l_z = 0$, $k_z = 0$ light hole energy eigenvalues as functions of the axial field $\boldsymbol{H}$ for $R = 50$ Å in an InSb-type semiconductor anti-wire. The values of m are $m = 0, \pm 1, \pm 2, \pm 3, -4, -5, -6$.

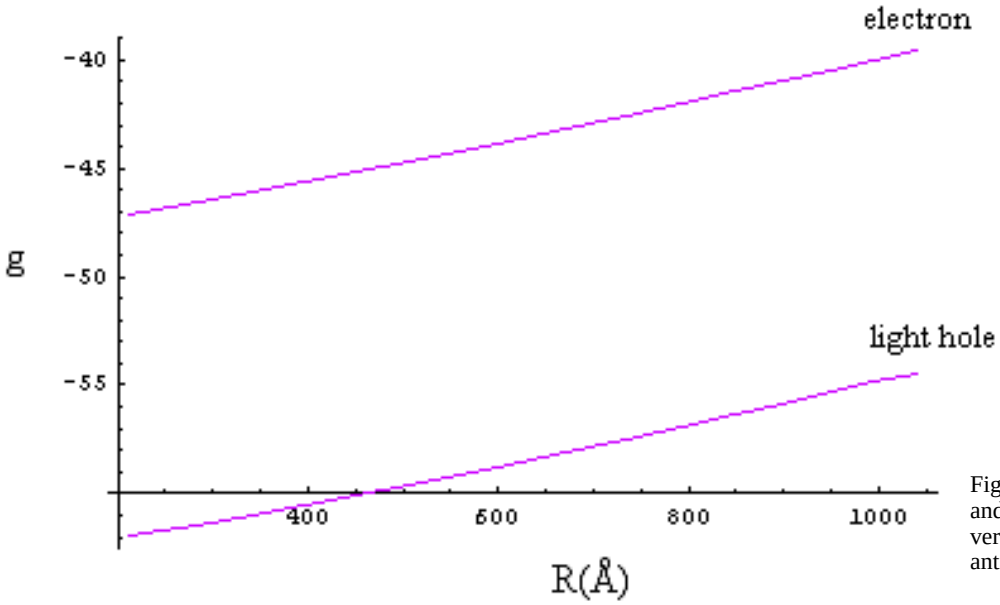

Fig. 4. The electrons and light holes g-factor versus the radius in an anti-wire of InSb.

spin positive values. These results agree well with the study of Masale [9].

Figure 3 shows the magnetic field change of the lowest order subbands for $l = 0$, $k_z = 0$ light hole energy eigenvalues in an InSb anti-wire of radius $R =$ 50 Å with infinite potential; the m values are $m = 0, \pm 1, \pm 2, \pm 3, -4, -5, -6$. The near-linearity variation of these energy subbands with the magnetic field for the radius 50 Å must be noted. In addition to this, it must also be noted that the $m \leq$

-2 states all fall in the infinitely degenerate ground state.

Figure 4 shows g-factor dependence on R for the fixed magnetic value $\boldsymbol{H} = 1$ T for electrons and light holes. As is seen in Fig. 4, with the decreasing R, the g-factor asymptotically approaches the respective bulk values for both electrons and light holes.

4. Conclusion

In this work, using Kane's three-band model, the spectrum of carriers with and without magnetic field and the electron and light hole effective g-factor for Kane-type semiconductor anti-wires are calculated. The nonparabolicity of the spectrum of electrons, light holes and spin-orbital splitting valence bands was taken into account. The effective g-factor was studied for the ground state as a function of the radius. The difference of the parabolic and nonparabolic band model in a zero magnetic field is represented.

[1] T. Chakraborty, Quantum Dots, Elsevier, Amsterdam 1999.
[2] D. Bimberg, M. Grundman, and M. Ledentsov, Quantum Dot Heterostructures, Wiley, New York 2001.
[3] N. C. Constantinou, M. Masale, and D. R. Tiley, J. Phys. Condens. Matter **4**, 4499 (1992).
[4] N. C. Constantinou, M. Masale, and D. R. Tiley, Phys. Rev. B **46**, 15432 (1992).
[5] D.-S. Chuu and C.-S. Wang, Physica B **202**, 118 (1994).
[6] W. Zawadski and M. Kubisa, Semicond. Sci. Technol. **8**, S240 (1993).
[7] A. A. Kiselev and E. L. Ivchenko, Pismo JETF **67**, 41 (1996).
[8] A. A. Kiselev, E. L. Ivchenko, and U. Rossler, Phys. Rev. B **58**, 16353 (1998).
[9] M. Masale, Physica B, **291**, 256 (2000).
[10] N. Aquino, E. Castano, and E. Ley-Koo, Chin. J. Phys. **41**, 276 (2003).
[11] R. Bowers and Y. Yafed, Phys. Rev. **115**, 1165 (1959).
[12] B. M. Askerov, Kinetic Effects in Semiconductors, Nauka, Leningrad 1970.
[13] A. I. Anselm, Introduction to Semiconductor Theory, Nauka, Moscow 1978; Prentice-Hall, Englewood Cliffs, NJ 1978.
[14] V. M. Galitskii, B. M. Karnakov, and V. I. Kogan, A Collection of Problems in Quantum Mechanics Science, Moscow 1981 (in Russian).
[15] Al. L. Efros and M. Rosen, Phys. Rev. B **58**, 7120 (1998).
[16] M. Abramovich and A. Stegun, Handbook of Mathematical Functions, Dover, New York 1965, p. 504.
[17] S. Çakmak, A. M. Babayev, E. Artunç, A. Kökce, and S. Çakmaktepe, Physica E **18**, 365 (2003).